

Zeitschrift: IABSE reports = Rapports AIPC = IVBH Berichte
Band: 66 (1992)

Artikel: Failure mechanisms in rotating bending fatigue on 7-wire strands
Autor: Gourmelon, Jean-Paul / Brevet, Pierre / Siegert, Dominique
DOI: <https://doi.org/10.5169/seals-50702>

Nutzungsbedingungen

Die ETH-Bibliothek ist die Anbieterin der digitalisierten Zeitschriften auf E-Periodica. Sie besitzt keine Urheberrechte an den Zeitschriften und ist nicht verantwortlich für deren Inhalte. Die Rechte liegen in der Regel bei den Herausgebern beziehungsweise den externen Rechteinhabern. Das Veröffentlichen von Bildern in Print- und Online-Publikationen sowie auf Social Media-Kanälen oder Webseiten ist nur mit vorheriger Genehmigung der Rechteinhaber erlaubt. [Mehr erfahren](#)

Conditions d'utilisation

L'ETH Library est le fournisseur des revues numérisées. Elle ne détient aucun droit d'auteur sur les revues et n'est pas responsable de leur contenu. En règle générale, les droits sont détenus par les éditeurs ou les détenteurs de droits externes. La reproduction d'images dans des publications imprimées ou en ligne ainsi que sur des canaux de médias sociaux ou des sites web n'est autorisée qu'avec l'accord préalable des détenteurs des droits. [En savoir plus](#)

Terms of use

The ETH Library is the provider of the digitised journals. It does not own any copyrights to the journals and is not responsible for their content. The rights usually lie with the publishers or the external rights holders. Publishing images in print and online publications, as well as on social media channels or websites, is only permitted with the prior consent of the rights holders. [Find out more](#)

Download PDF: 05.09.2025

ETH-Bibliothek Zürich, E-Periodica, <https://www.e-periodica.ch>

Failure Mechanisms in Rotating Bending Fatigue on 7-Wire Strands

Mécanismes de rupture par fatigue en flexion rotative de torons 7 fils

Bruchmechanismus bei Drehbiegebeanspruchung siebendrähtiger Litzen

Jean-Paul GOURMELON

Ingénieur en Chef
Lab. Central Ponts et Chaussées
Bouguenais, France

Pierre BREVET

Ingénieur ECL
Lab. Central Ponts et Chaussées
Bouguenais, France

Dominique SIEGERT

Ingénieur TPE
Lab. Central Ponts et Chaussées
Bouguenais, France

Jean-Paul Gourmelon, born in 1938, graduated from Ecole Nationale des Travaux Publics de l'Etat (1962) and Ecole Nationale des Ponts et Chaussées (1971). With the LCPC since 1971, he was head of the Metal Construction and Cables Division (1986-1991). He is currently deputy technical director for civil engineering structures.

Pierre Brevet, born in 1946, graduated from Ecole Centrale de Lyon (1968) and was awarded Doctor Ingénieur (Lyon University 1973). With the LCPC since 1974, he is currently head of the Cables Behaviour and Metal Appraisalment Section.

Dominique Siegert, born in 1965, engineer from Paris Nord University (1989) and Ingénieur des Travaux Publics de l'Etat (1991). With LCPC since 1991, he is currently research engineer at the Cables Behaviour and Metal Appraisalment Section.

SUMMARY

In order to study the behaviour of prestressing strands subjected to bending fatigue, the authors applied a mathematical model to calculate the stay distortion near the anchorage. They reproduced on an original rotating bending test apparatus such curvatures representative of onsite conditions. Behaviour of non-coated and galvanized strands is given and cracking initiation mechanism by fretting is presented. Influence of corrosive surrounding is also shown.

RÉSUMÉ

En vue d'une étude technologique du comportement de torons de précontrainte soumis à la fatigue par flexion, les auteurs ont appliqué un modèle mathématique pour calculer la déformée d'un hauban au voisinage de l'ancrage puis reproduit sur une machine de flexion originale des courbures représentatives des conditions sur site. Les comportements de torons non revêtus et de torons galvanisés sont donnés et le mécanisme d'amorçage des fissures par fretting est mis en évidence. L'influence d'un environnement corrosif est également montré.

ZUSAMMENFASSUNG

Im Rahmen einer technischen Studie zum Ermüdungsverhalten von Vorspannlitzen unter Biegebeanspruchung untersuchten die Verfasser realistische Krümmungsradien in einem Drehbiegeversuchsstand. Dazu wurden vorgängig mit einem mathematischen Modell die Verformungen von Schrägseilen in der Nähe ihrer Verankerung ermittelt. Berichtet wird von Verhalten unbeschichteter und galvanisierter Litzen, wobei die Rißentstehung unter Reibermüdung und der Einfluß einer korrosiven Umgebung dargestellt werden.



1. INTRODUCTION

Cable stayed or reinforced civil engineering structures use either mono-strand cables (helical or lock-coil) either parallel wires cables or parallel strands cables.

The latter are generally made of prestressing strands clamped one by one. Initially used for prestressed concrete constructions those cables where fully buried inside concrete ; their applications for stay cables are quite new and under fast development for large span cable-stayed bridges (Normandy Bridge ...).

In such structures, in addition to the random sollicitations due to traffic, climatic effects (rain, wind ...) produce alternate and repeated bending deformations at the anchorages level of cables, inducing fatigue phenomena.

It appears, then, useful to know under laboratory conditions the bending fatigue effects on basic strands. After modelling the bending conditions on site and describing the test apparatus, results of first technological tests and fractures analysis are presented using an initial damaging mechanism by fretting.

2. MODELLING THE DISTORTION OF A STAY CABLE

In order to know the actual sollicitations on stays and specially the bending amplitude near the anchorages three approaches can be taken :

- 1) measuring distortions on an actual bridge under traffic. These measures are not reliable enough for giving significant curvature values.
- 2) measuring in laboratory distortions of a cable under known sollicitations. These measures, made on prestressing strands are, to date, determined with quite a large uncertainty ($\approx 100\%$) due to the fact that the expected deformations have small amplitudes and are located near the anchorages.
- 3) calculation of local deformations of a cable using a model where boundary conditions and parameters are issued from experimental estimations. Such a model has been developped in order to give curvature values consistent with experimental values and with the natural continuous variation of this parameter for actual materials.

2.1 Description of the model

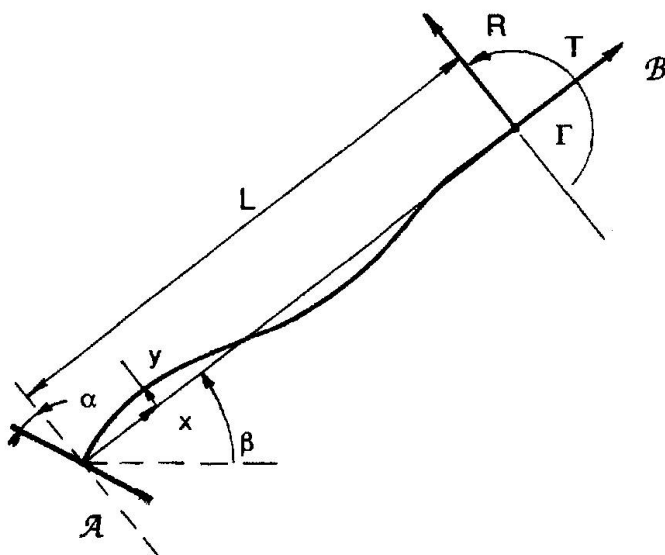


Fig. 1

The cable is modelled as a beam with a constant stiffness modulus, subjected to an axial tensile strength and embedded at each end. The lower embedment A is rotated with an amplitude α from the acting line of the stay.

The material mass is taken into account in the distortion calculation but its influence on the axial tensile strength variation is neglected (the stay cable being inclined with an angle β from the horizontal line).

Such a model gives results of curvatures slightly greater than those given by the model of semi-infinite cable without mass (Gimsing [1]) and is based on the classical equation (K.G. Mc Connel and W.P. Zemke [2]) :

$$EI \frac{\delta^2 y}{\delta x^2} - T y + \frac{mg \cos \beta}{2} (b - x)^2 - R (l - x) + \Gamma = 0$$

where :

- El actual stiffness modulus,
- T axial tensile load applied to the cable,
- β stay slope angle,
- R reaction of the embedment (right side) *
- Γ embedment torque (right side) *

* hyperstatic unknown parameters

and for which the solution is given by

$$y(x) = L_1 \exp(w * x) + L_2 \exp(-w * x) + A x^2 + B x + C$$

with $w = \sqrt{T/EI}$

The L_1 , L_2 , A, B, C, coefficients are determined from the boundary conditions, taking into account the particular solution giving B and C depending of L_1 and L_2 , with $A = mg/2T$.

2.2 Numerical results

Many numerical applications of the above model have been made on cables from 12.6 to 85 millimetres diameter. A good agreement is obtained between experimental and theoretical distortions for the largest cables. On the contrary, as we said, measures on low stiffness cables (low diameter) are not accurate enough for a direct validation of the calculation.

The following results refer to a 7 wire-strand, 12.6 mm diameter, for which the stiffness has been estimated according to the approximations given by G.A. Costello ($EI = 21.2 \text{ Nm}^2$, interwires full-slip ; $EI = 247 \text{ Nm}^2$, interwires no-slip) [3] and measured on an embedded beam ($EI = 107 \text{ Nm}^2$).

Table 1 gives the maximal curvature radius, calculated at the embedding level \mathcal{A} for anchorage rotation angles consistent with the deck distortions of a bridge and with the construction accuracy of the anchorages alignment with the stay.

α (degrees)	$\beta = 45^\circ$	$\beta = 0^\circ$		
	$EI = 107 \text{ Nm}^2$	$EI = 107 \text{ Nm}^2$		$EI = 247 \text{ Nm}^2$
	L = 100	L = 100	L = 10	L = 10
- 0.1	(-) 20.2	(-) 13.3	31.7	48.0
+ 0.1	(-) 7.2	(-) 5.6	(-) 17.2	(-) 26.1
+ 0.5	(-) 3.1	(-) 2.8	(-) 4.2	(-) 6.4
+ 1.0			(-) 2.1	(-) 3.3
+ 2.0			(-) 1.1	(-) 1.7
+ 2.5			(-) 0.8	(-) 1.3

Table 1 Curvature radius (metre) calculated for a 12.6 strand under 78 kN tensile load

3. EXPERIMENTAL APPLICATIONS

The execution of bending rotating tests where carried out, reproducing curvatures of the same order of magnitude as those calculated above. These tests allow the determination of an endurance limit for the strands.

A scheme of the apparatus is given in Figure 2 : the sample with a free length L is embedded at each end in anchorages (\mathcal{A} and \mathcal{B}) symmetrically driven into rotation around the X axis. Bending is obtained by nearing the two anchorages which are free in rotation around the Z axis, perpendicular to the XY plan.

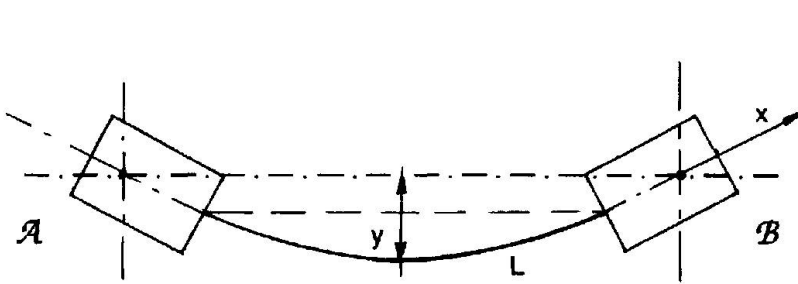


Fig. 2 Scheme of test apparatus

The sample itself bears inside the anchorages so that, in this zone, slipping between the central wire and the six external wires is impeded.

The tests were carried out on non-coated steel and galvanized steel strands, in the open air or with partial dipping in artificial seawater. Test frequency allowing the conjugate action of the mechanical fatigue solicitation and of the surrounding corrosiveness was 0.26 Hz.

Results obtained with the "K non-broken samples method" [4] (with $K=3$) are shown in Figures 3 and 4. The "curvature radius" parameter is chosen in order to make easier the application of the results to in site checking operations on bridges.

Notice that the new strands (non-coated or galvanized) show an endurance limit. The oxidized strands (pits deepness around 2/10 mm.), under the same experimental conditions, also show an endurance limit. But conjugate action of fatigue and corrosion does not reveal the existence of this threshold.

It is noted a large scattering for the galvanized strands behaviour when in corrosive surrounding A3 and, for the lowest lifetimes (700 000 cycles) a lack of difference in lifetime with or without this surrounding.

4. PRESTRESSING STRANDS BEHAVIOUR ANALYSIS BY ROTATING BENDING FATIGUE

Experimental behaviour described in the above chapter, particularly the better behaviour of galvanized steels for long lifetimes involves the knowledge of cracking initiation mechanisms under rotating bending, all the more so because galvanizing does not bring any improvement in fatigue behaviour for high strength steels [5].

Analysis of "corrosion" products extracted from strands after tests, macrographic investigation on fractures and surfaces of strand wires and study of the wires behaviour under fretting enabled a justification for the observed behaviours.

4.1 Fatigue fracture of oxyded strands

Investigations of strands fractures subjected to fatigue after corrosion by a storing in natural atmosphere show that the external wires are the first to be harmed by cracking and fracture. Fatigue cracks are initiated on corrosion pits, the measured deepness of which is $2.7 \cdot 10^{-3} \pm 0.2 \cdot 10^{-3}$ millimetres.

4.2 Fatigue fracture of non-coated and galvanized strands

The first peripheral wire breaks are sometimes preceded by the central wire break. For the tests with a fatigue lifetime around two millions cycles, the central wire is always broken.

Strands fracture is preceded by production of oxyded powders, red for non-coated strands, black for galvanized strands. The analyses of powders by X-Ray diffractometry (or Mossbauer spectrometry) show out :

– for red powder

Iron	Fe
Iron oxide	Fe ₂ O ₃ (hematite)
Iron oxide	FeO (wüstite) – traces

– for black powder

Zinc	Zn
Zinc oxide	ZnO
Iron oxide	Fe ₂ O ₃ (hematite)

Those powders are typical of a fretting wear phenomenon producing metal particles with large reactive surfaces, inducing fast oxidation and oxides presence in the collected powders.

The investigation of wires surface (figure 5) well shows metal tearings at interwire contacts, and especially at central wire/peripheral wires contact. Fracture initiations themselves correspond geometrically to interwire contacts (figure 6), this allowing to state that frictions are the source of fractures (fretting fatigue).

4.3 Fracture under conjugate action of fatigue and corrosion

The common characteristic of all tests carried out under these conditions is the multiple fractures obtained on a same wire and the very close cracking observed at the interwires contacts (figure 7).

For galvanized strands, cracking and fractures are preceded by zinc dissolving and/or complete wearing.

Analysis of corrosion and wearing products by X-Ray diffractometry does not clearly exhibit any presence of iron or zinc under metallic form. The identified crystallized products are :

– for non-coated strands

Goethite	α FeOOH
Akaganeite	β FeOOH
Magnetite	Fe ₃ O ₄

– for galvanized strands

Carbonate "Type 1"	2ZnCO ₃ ,3Zn(OH) ₂
Carbonate "Type 2"	ZnCO ₃ ,3Zn(OH) ₂ ,H ₂ O
Chloride	ZnCl ₂ ,4Zn(OH) ₂
Nickel-Iron basic carbonate	

Lack of iron and zinc detection is due to :

- either diffraction lines superposition for these metals and their corrosion products,
- or corrosiveness of the A3 surrounding, inducing complete oxydation of particles teared from friction zones.

5. INTERPRETATION

Fractures of prestressing strands subjected to rotating bending fatigue tests with or without corrosive surrounding are initiated, for the least hard solicitations, at the interwires contacts (central wire/peripheral wires or peripheral wires/peripheral wires).

Analysis and investigations show that fretting wear and fatigue mechanisms initiate fatigue cracks inducing fracture.

Zinc favourable effect on fatigue behaviour is connected to this fretting mechanism. It has been earlier demonstrated [6] that galvanizing zinc delays wearing of basic steel at interwires contacts, and then initiation of surface damages inducing fatigue fractures.

For galvanized strands subjected simultaneously to fatigue solicitations and to A3 surrounding corrosive action, the same process due to zinc action delaying surface damaging can be kept in mind. It explains the equivalent lifetimes with or without corrosive surrounding observed for the hardest mechanical conditions shown on figure 4 (700000 cycles for fracture). This mechanism explains also the scattering observed for tests under less hard conditions ; zinc dissolving phenomena are indeed miscontrolled during long time tests (temperature, surrounding concentration, corrosion products disposal ...) so that destroying kinetics of galvanizing zinc is not the same from one test to the other.

Multiple cracks and fractures under the action of fatigue coupled with corrosion are simply explained by comparison of defects and surface cracks density on figures 5 and 7. Cracks initiations are directly related to short cracks due to fretting mechanisms. In fretting phenomena wear or fatigue begins by surface short cracks development [7,8]. These ones, inclined around 45°, grow inducing :

- either surface chipping (wear),
- or, under corrosive surrounding and overall fatigue solicitations, cracks perpendicular to the main stress direction.



Action of corrosive surrounding being mainly strong on the new metal surfaces created at the short cracks level helps these fatigue cracks to grow (dissolving, embrittlement, mechanical effects of corrosion salts on cracks opening ...).

6. CONCLUSIONS

The rotating bending fatigue behaviour of prestressing strands near the endurance limit is related to interwire friction phenomena (fretting). Wear results in surface defects inducing cracks initiation. The action of corrosive surrounding helps cracking.

Favourable zinc action is also related with fretting phenomena. This material acts in interwires contacts as a third-body (wearing material) which delays basic steel damaging.

From this study it appears also that the curvature radius, calculated for on site anchorages misalignment or rotations of one or two degrees, are of the same order of magnitude as those corresponding to the endurance limit of strands constituting stays. Particular attention to stays installation should minimize fatigue fracture risks.

REFERENCES

1. GIMSING N.J., Cable Supported Bridges – Concept and Design. Wiley Intersciences, 1983.
2. Mc CONNEL K.G. – ZEMKE W.P., Experimental Mechanics
3. COSTELLO G.A., Theory of wire rope, Springer Verlag, 1990.
4. LIEURADE H.P. et la Commission "Fatigue des métaux" de la S.F.M., PYC Editions, 1982.
5. BERGERGREN Y. – MELANDER A., An experimental and theoritical study of fatigue properties of hot-dip-galvanized high-strength sheet steel, Int. J. Fatigue, May 1992, pp. 154–162.
6. BREVET P., Effet des frottements cycliques sur la durée de vie des câbles pour ouvrages d'art, Bull. Liaison Labo P & Ch. N° 166, Mars–Avril 1990.
7. BILL R.C., Fretting wear and fretting fatigue, how are they related ?, ASME JOLT, N° 105, 1983, pp. 230–238.
8. BERTHIER Y., Mecanismes et Tribologie, Thèse Docteur–es–Sciences, Lyon Juillet 1988, N° 88 ISAL 0050.

ANNEXE

A3 Reagent

6 g/l	MgCl	Magnesium Chloride
30 g/l	NaCl	Sodium Chloride
1,9 g/l	Na ₂ HPO ₄	Phosphate of Sodium
12,5 g/l	H ₃ BO ₃	Boracic Acid
pH 8	Na ₂ CO ₃	Sodium Carbonate Q.S.P.

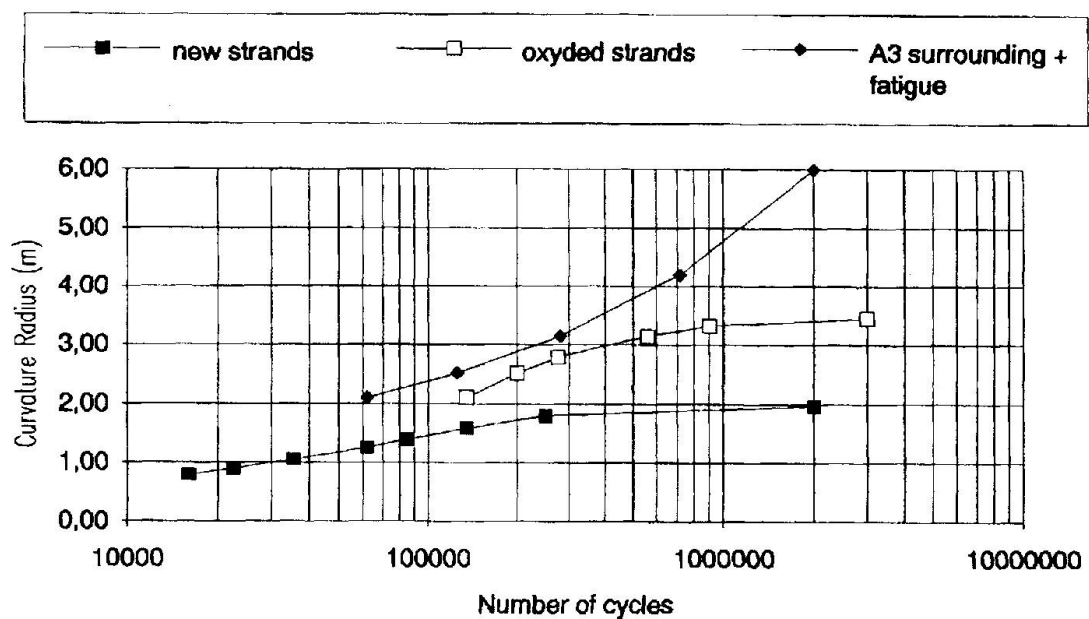


Fig.3 Results on non-coated strands 12.6 mm diameter

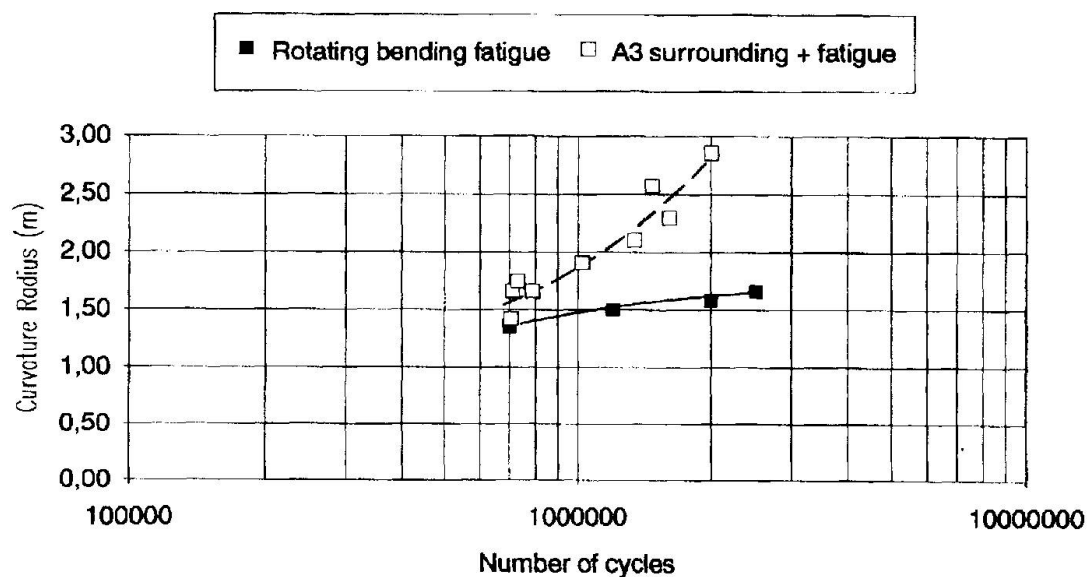


Fig.4 Results on galvanized strands 12.6 mm diameter

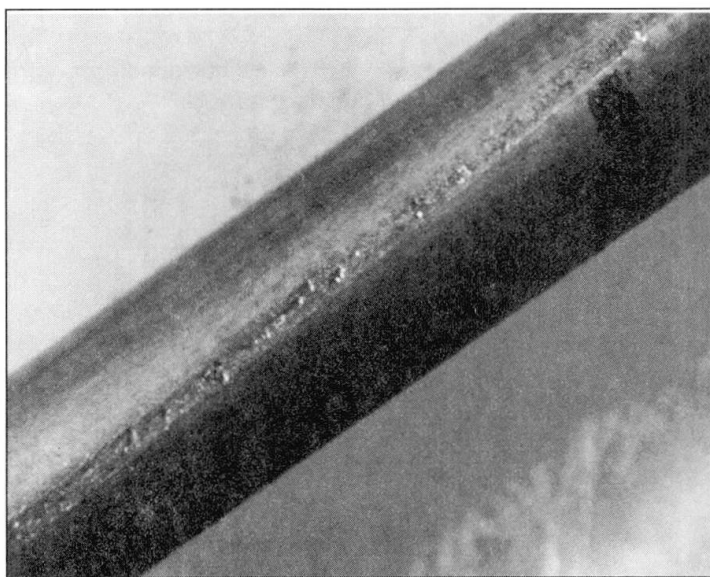


Fig. 5 Particles tearing at interwire contacts (500000 cycles)

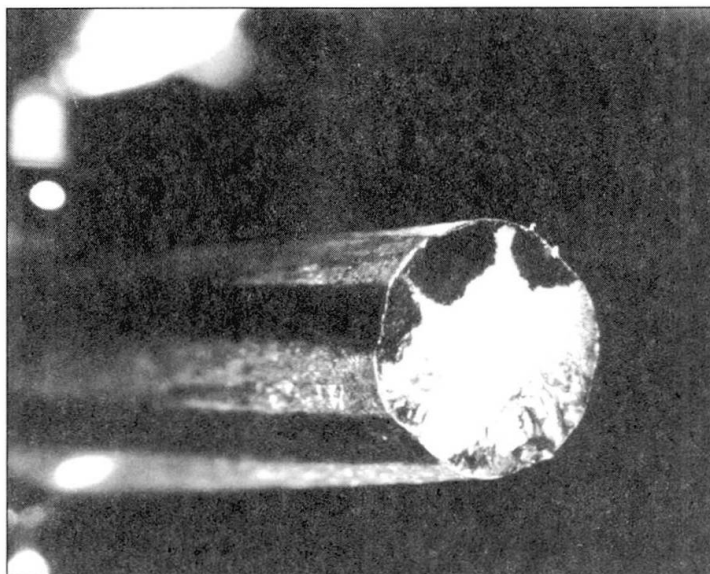


Fig. 6 Correspondance between interwire contacts and cracking initiation (strand core)

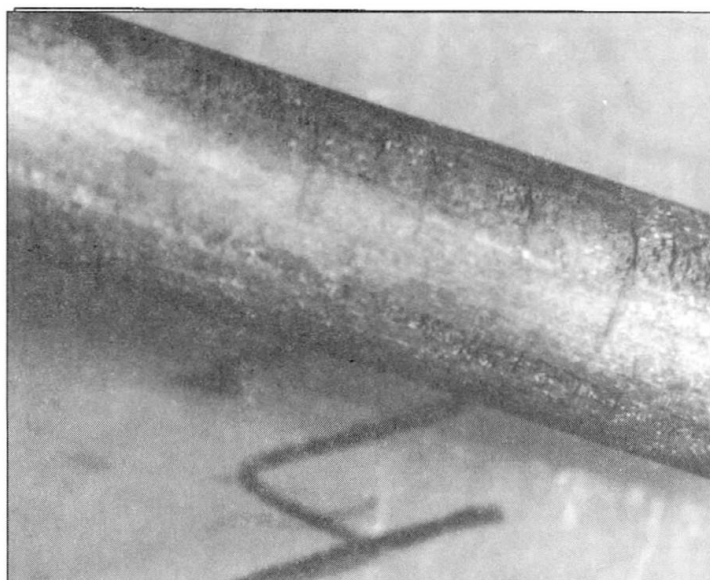


Fig. 7 Cracks under interwire contacts with conjugate action of fatigue and corrosive surrounding